Intensity-modulated radiation therapy in head and neck cancers:The Mallinckrodt experience

ARTICLE *in* INTERNATIONAL JOURNAL OF CANCER · APRIL 2000

Impact Factor: 5.09 · DOI: 10.1002/(SICI)1097-0215(20000420)90:2<92::AID-IJC5>3.0.CO;2-9 · Source: PubMed

4 AUTHORS, INCLUDING:

Daniel Low
University of California, Los Angeles
656 PUBLICATIONS **11,852** CITATIONS
SEE PROFILE

Carlos A Perez
Washington University in St. Louis
610 PUBLICATIONS **19,322** CITATIONS
SEE PROFILE

Int. J. Cancer (Radiat. Oncol. Invest): **90,** 92–103 (2000)

Publication of the International Union Against Cancer

Intensity-Modulated Radiation Therapy in Head and Neck Cancers: *The Mallinckrodt Experience*

K.S. Clifford Chao, M.D.,* Daniel A. Low, Ph.D., Carlos A. Perez, M.D., and James A. Purdy, Ph.D.
Radiation Oncology Center, Mallinckrodt Institute of Radiology, Washington University Medical Center, St. Louis, Missouri

SUMMARY **The purpose of the study was to investigate the feasibility and the optimization of tomotherapy-based intensity-modulated radiation therapy (IMRT) in patients with head and neck cancer. From February 1997 to November 1997, 17 patients with squamous cell carcinoma of the head and neck were treated with IMRT. Patients were immobilized with a noninvasive mask and treated using a serial tomotherapy device on a 6 MV linear accelerator. Treatment planning was performed on a Peacock inverse planning system and prescription optimization was used to achieve the best plan for target coverage and parotid sparing. The treatment planning system process has a dosimetric characteristic of delivering different doses to different target structures simultaneously in each daily treatment; therefore, the biological equivalent dose was implemented using the linear-quadratic model to adjust the total dose to the target volume receiving a daily dose of less than 1.9 Gy. All eight patients with gross disease (six in the nasopharynx, two in the tonsil) and one patient with recurrent nasopharyngeal carcinoma received concurrent cisplatin chemotherapy. Six postoperative patients were treated with irradiation alone. Median follow-up was 2.2 years (range 2.6–1.8 years). All patients completed the prescribed treatment without unexpected interruption. Acute side effects were comparable to those of patients treated with conventional beam arrangements during the same period. No patient required gastrostomy during irradiation. The preliminary experience showed that the noninvasive immobilization mask yielded high positioning reproducibility for our patients. To spare the parotid gland, which is in the proximity of the target, a fraction of the target volume may not receive the prescribed dose. In the best-achievable plan of our studied cohort, only 27% ± 8% of parotid gland volumes were treated to more than 30 Gy, while an average of 3.3% ± 0.6% of the target volume received less than 95% of the prescribed dose. This is mainly related to the steep dose gradient in the region where the target abuts the parotid gland. The inverse planning system allowed us the freedom of weighting normal tissue-sparing and target coverage to select the best-achievable plan. Local control was achieved in eight patients with gross tumor; six were treated postoperatively. Of three reirradiated patients, two had symptomatic improvement but persistent disease, and one is without evidence of disease. In summary, a system for patient immobilization, setup verification, and dose optimization for head and neck cancer with parotid sparing without significantly compromising target coverage is being implemented for a tomotherapy-based IMRT plan at the Mallinckrodt Institute of Radiology. The initial clinical experience in tumor control is promising, and no severe adverse acute side effects have been observed. Further refining of delivery technology and the inverse planning system, gaining clinical experience to address target definition and dose inhomogeneity within the targets, and understanding the partial volume effect on normal tissue tolerance are needed for IMRT to excel in the treatment of head and neck cancer.** *Int. J. Cancer (Radiat. Oncol. Invest.) 90, 92–103, (2000).* **© 2000 Wiley-Liss, Inc.**

*Correspondence to: K.S. Clifford Chao, M.D., Radiation Oncology Center, Box 8224, Washington University Medical School, 4939 Children's Place, Ste. 5500, St. Louis, MO 63110. Phone: (314) 362-8502; Fax: (314) 362-8521; E-mail: chao@radonc.wustl.edu

Received 13 January 2000; Revised 18 February 2000; Accepted 24 February 2000

Key words: head and neck cancers; intensity-modulated radiation therapy

INTRODUCTION

Head and neck cancers are devastating and life-threatening. In 1997, approximately 70,000 new cases were diagnosed in the United States, and 20,000 persons died of the disease [1]. As our medical knowledge and technology in the treatment of this disease advance, and through the use of multidisciplinary approaches, more lives are being saved or prolonged. Radiation therapy has become one of the basic components of multidisciplinary treatment. When appropriately integrated with other modalities (surgery, chemotherapy) or selectively given as definitive therapy, local tumor control can be obtained.

Several critical organs in the head and neck region are usually in close proximity to the tumor. This spatial characteristic makes radiation therapy for head and neck cancers a very challenging task. For example, tumors originating in the pharyngeal wall are usually concave and wrap around the spinal cord, and the parotid gland is in proximity to the lymph nodes, which are usually involved; tumors arising from the paranasal sinuses often invade the space adjacent to the optic nerves or optic chiasm. Radiation doses that these critical organs can receive without causing complications lie in the range of 30–60 Gy [2]; however, the dose needed to control gross tumor often exceeds 70 Gy. With the development of an advanced form of three-dimensional conformal radiation therapy (3D CRT), called intensity-modulated radiation therapy (IMRT), the ability to deliver tumor doses to the target volume while maintaining low doses to the critical organs now appears achievable [3].

IMRT is capable of generating complex 3D dose distributions to conform closely to the target volume even in tumors with concave features. With IMRT, the beam intensity (fluence) is optimized as it is oriented around the patient using computer algorithms. This form of computer algorithm considers not only the target and normal tissue dimensions but also user-defined constraints such as dose limits. This process is based on the "inverse method" of treatment planning and is capable of generating significant dose gradients between the target volume and adjacent tissue structures to accomplish the intended dose–volume prescription [4]. Because of this specific feature, a precise mechanical system to deliver and validate the intended radiation dose to the desired area is crucial. An inverse prescription guideline that optimizes tumor target coverage and normal tissue-sparing is another pertinent component of IMRT treatment. In this report, we describe our initial experience in implementing a tomotherapy-based IMRT system for head and neck cancer treatment at the Mallinckrodt Institute of Radiology, Washington University School of Medicine, St. Louis, Missouri.

MATERIALS AND METHODS

From February 1997 to November 1997, 17 patients with squamous cell carcinoma of the head and neck were treated with tomotherapy-based IMRT at the Mallinckrodt Institute of Radiology. Ages ranged from 42–75 years. There were two Black, two Asian, and 13 White patients. The location of the primary tumor was the nasopharynx in seven patients, oropharynx in seven, and supraglottic larynx in one. Additionally, two patients presented with metastatic squamous cell carcinoma in the upper and midcervical nodes from an unknown primary tumor. Seven patients with nasopharyngeal carcinoma and two patients with tonsillar carcinoma were treated with concurrent cisplatin chemotherapy (80–100 mg/m^2 every 3 weeks) during radiation therapy. Six postoperative cases were treated with radiation therapy alone. Median follow-up was 2.2 years (range 2.6–1.8 years).

Immobilization and Image Acquisition

We elected to use a noninvasive immobilization method with the patient placed in the supine position on a custom-made head support and a reinforced thermoplastic immobilization mask around the head (Fig. 1). This procedure allowed precise repositioning over the course of treatment. A volumetric computed tomography (CT) image was acquired with the patient immobilized in the treatment position from our dedicated CT simulator (Picker AcQsim; Picker International, St. Davids, PA) and the data were transferred to an inverse planning system (Peacock treatment planning system; NOMOS Corp., Sewickley, Pa.). The scan slice thickness was 3 mm throughout the region containing the tumor target. Regions superior and inferior to the tumor target were scanned with a slice thickness of 5 mm. Intended target volumes representing gross and microscopic tumor and organs at risk were defined on the prescription page of the inverse planning system. Structures encompassed in the irradiation region were contoured on

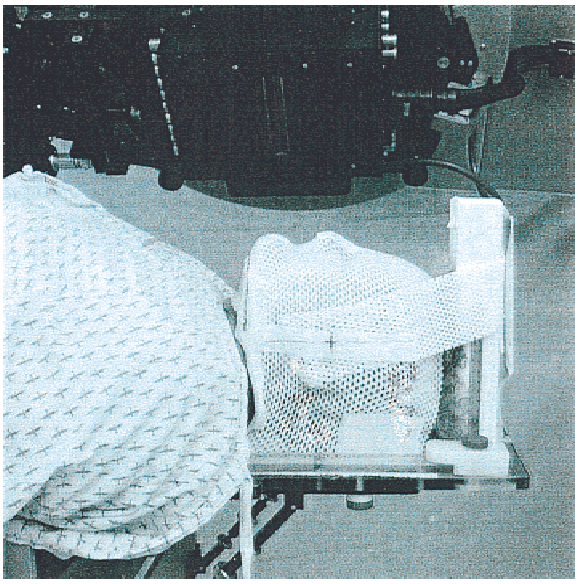

Fig. 1. Noninvasive immobilization system for intensity-modulated radiation therapy. The patient was placed in the supine position on a custom-made head support with a reinforced thermoplastic immobilization mask.

multiple consecutive CT scans. One specification used in this contouring process is illustrated in Figure 2. The definition of "target volume" for tumor or tumor bed in the inverse planning system resembles the concept of gross target volume (GTV) and clinical target volume (CTV) as described in the International Commission on Radiation Units (ICRU) Report #50 [5]. GTV was defined based on diagnostic imaging, usually named "target 1." The GTV included gross tumor and its residing anatomical compartment, such as nasopharynx, oropharynx, or Level II lymph node regions [6]. The microscopic risk area (CTV) was usually named "target 2" or "target 3" for different prescription doses, and the target volume was defined by the anatomical compartment at risk according to the nature of tumor spread or the pathological features in the surgical specimen. However, the system did not allow defining a margin to establish a planning target volume (PTV) for patient setup uncertainty and organ motion; instead, it provided for specifying a "tissue growth" column on the prescription page.

Prescription Dose

The desired minimum dose to target(s) and the maximum allowable dose to nontarget structures were defined in the prescription. These parameters were used as the goals in designing an optimized plan. However, it was not always possible to meet both the dose to the targets and the dose limit to the

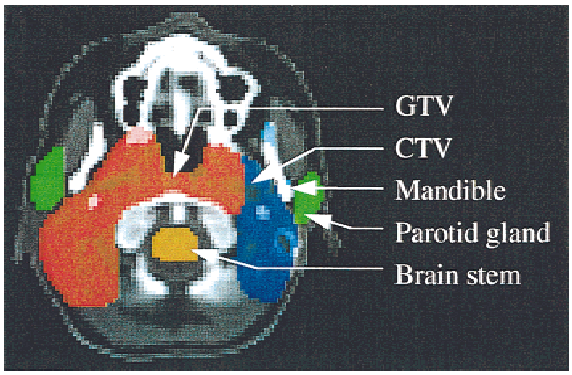

Fig. 2. Target definition for head and neck intensity-modulated radiation therapy.

nontarget normal structures; thus, adjustments in the input parameters were required. In addition to the dose, several other parameters were also specified in the prescription page for treatment optimization:

- Growth: Structure growth is similar to the PTV concept in ICRU #50. An optional growth margin for each target and nontarget structure can be assigned. The target or tissue growth is incorporated into consideration for fluence optimization, but is not shown in the dose–volume histogram (DVH) display. Therefore, the results illustrated in this study pertain to the CTV coverage.
- Weight: A structure weight (from 0–2) was assigned for each target and nontarget structure to indicate its relative importance to other structures. As the default, a target can be weighted 1 and then other structures can be assigned to 0 (not important at all), 0.5 (less important than target), 1 (as important as target), or greater than 1 (more important than the target).
- Target priority: As a result of adding margin(s) around target(s) and nontarget structures, adjacent structures/targets might overlap. The Peacock system did not allow multiple structure assignments to pixels during optimization. The Peacock system uses a check-mark for each individual structure to signify whether the target or the adjacent structure was selected when they overlapped.

The beam fluence intensity was determined by computer optimization to produce the best conformal plan in accordance with the above parameters and dose specification. The optimization was conducted on the target volume including margin (growth), but the dose statistics displayed (including DVHs) were based on the target volume alone.

Table 1. IMRT Target Dose Specification with Biological Equivalent Dose (BED) Correction at Washington University

		IMRT Prescription		
Target volume	Correctional dose/fraction	Gross tumor* (37 fractions)	High-risk postoperative (35 fractions)	Intermediate-risk postoperative (32 fractions)
Low-risk	50.4/1.8 Gy	55.5/1.5 Gy	54.25/1.55 Gy	52.8/1.65 Gy
Intermediate-risk	59.4/1.8 Gy	62.9/1.7 Gy	61.25/1.75 Gy	60.8/1.9 Gy
High-risk (postoperative)	66.6/1.8 Gy	—	66.5/1.9 Gy	—
Gross tumor	70.2/1.8 Gy	70.3/1.9 Gy	—	—

*Patients received concurrent cisplatin (80–100 mg/m^2/q 3 w).
IMRT = intensity-modulated radiation therapy.

Dose Specification

The isocenter of each treatment segment may not be located within the target. Instead, the isocenter merely serves as the geometric center of each rotating arc for this tomotherapy-based IMRT. Therefore, the dose was specified to each target volume. Because concurrent chemotherapy was used in a substantial portion (9 of 17) of our patients, to avoid unexpected toxicity the daily fraction dose to the targets was defaulted at 1.9 Gy, five fractions per week. The maximum dose within the targets was designed not to exceed the prescribed dose by more than 15% (dose inhomogeneity $\leq$15%).

Another dosimetric characteristic of this form of IMRT is that different doses to different target structures can be delivered simultaneously in each daily treatment. For example, to design a treatment plan to deliver 1.9 Gy per day to the first target for a total of 70.3 Gy in 37 fractions and also treat another adjacent target that may contain microscopic disease to a minimum of 50.4 Gy in 37 fractions would result in a daily fraction size of only 1.36 Gy to the second target. Therefore, the concept of biological equivalent dose (BED) using a linear-quadratic model was implemented to adjust the dose to targets [7]. An α/β ratio of 10 Gy was used for BED conversion for tumor targets. Based on the tumor burden, target doses were defined into four categories based on our institutional treatment guidelines. *Low-risk regions* included primarily a prophylactically treated neck. *Intermediate-risk regions* were those adjacent to the *gross tumor* but not directly involved by tumor. *High-risk regions* included the surgical bed with soft tissue invasion by the tumor or extracapsular extension by metastatic neck nodes. Table 1 shows examples of dose prescriptions. Prescribed fraction size for the primary target was increased to 1.9 Gy in order to increase the minimal fraction size in the lower-risk region to 1.5 Gy. During this period of initial clinical experience, we encountered an increasing application of concurrent chemoirradiation promoted by a positive clinical outcome in a multicenter clinical study and meta-analysis [8,9]. To avoid unexpected late toxicity that may be associated with a high daily fraction size, we elected to constrain gross tumor fraction to 1.9 Gy. Because most of the gross tumors were either nasopharyngeal or tonsil primary tumors, the doses to the subclinical area delivered with IMRT in the upper head and neck region were more than 60 Gy and in 1.7 Gy daily fractions. Only small portions of the contralateral posterior neck received 1.5 Gy daily fractions, and the majority of the low-risk regions were in the lower neck, which was treated with a conventional technique at 1.8 to 1.9 Gy daily fractions.

Table 2. Normal Tissue Tolerance for IMRT Prescription

Organ	Tolerance (whole organ)
Optic nerve and optic chiasm	55 Gy
Retina	45 Gy
Brain stem	50–55 Gy
Spinal cord	45–48 Gy
Parotid gland	20–30 Gy
Mandible	70 Gy

IMRT = intensity-modulated radiation therapy.

Guidelines for Normal Tissue Dose/Volume Prescription

Normal organ structures, including brain, brain stem, spinal cord, lens, retina, optic nerves, optic chiasm, parotid gland, mandible, and glottis, were contoured on multiple CT scans. Tissue within the skin boundary but not included in critical normal structures or targets was designated as "unspecified tissue."

Guidelines for dose–volume tolerance when the organ was not encompassed in any tumor target for these 17 patients are shown in Table 2. DVHs

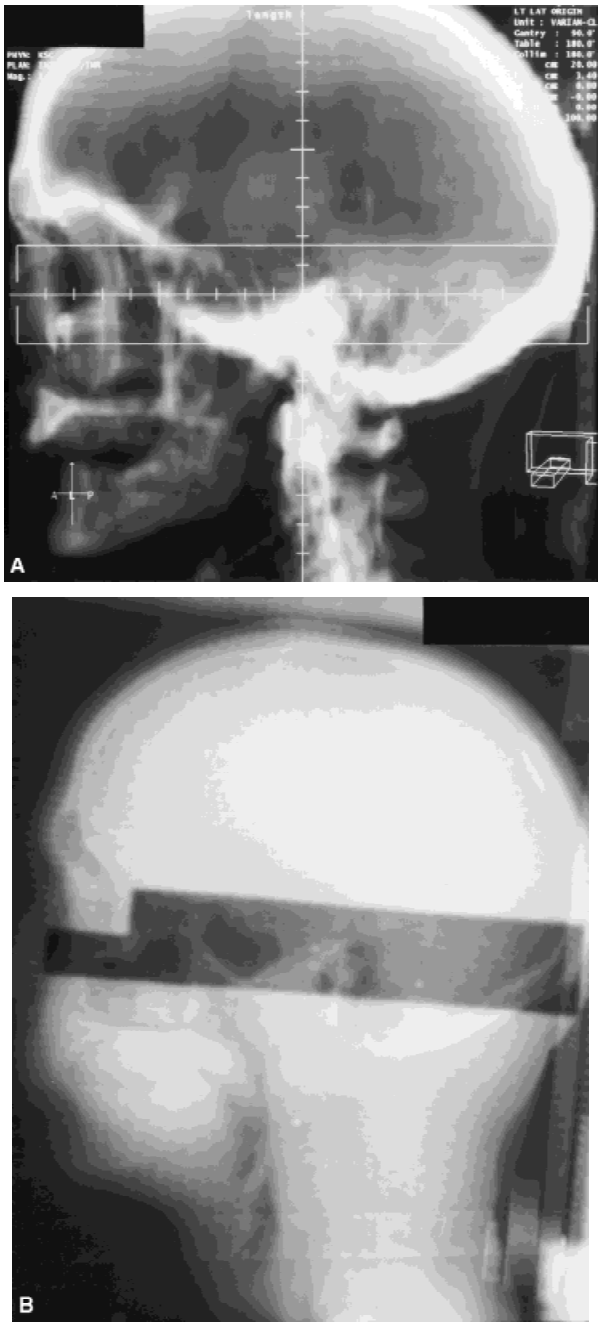

Fig. 3. **A**: A digitally reconstructed radiograph of lateral projection depicts a representative arc through nasopharynx and sphenoid sinus. **B**: A double-exposure portal film taken at the same geometry from the linear accelerator corresponds to the digitally reconstructed radiograph.

were generated for all critical normal structures and unspecified tissues.

Quality Assurance for Patient Setup Error

Lateral and anterior–posterior digitally reconstructed radiographs (DRRs) of the patient's head in the treatment position were generated on a CT simulation workstation (Fig. 3a). The multivane intensity modulated collimator (MIMiC, Nomos Corp., Sewickley, PA) was used for radiation delivery. Before each daily treatment, 1.6-cm wide strip portal films, centered at the plan origin, were obtained at 180° and 90° gantry angles and were compared with corresponding DRRs to ensure satisfactory reproduction of patient immobilization. Each segment was treated per prescription. For a better outline of head and neck anatomy, double-

Table 3. Prescribed and Delivered Doses to the Target and Parotid Gland

Target characteristics (no. of patients)	Prescribed dose*	Target dose (Gy)*			Parotid dose (Gy)*		
		Minimum	Mean	Maximum	Minimum	Mean	Maximum
Gross tumor (8)	70.48 ± 0.54	44.77 ± 11.93	72.49 ± 1.66	79.40 ± 2.2	8.10 ± 6.81	22.42 ± 5.22	60.66 ± 11.07
Postoperative (6)	64.18 ± 3.16	46.22 ± 11.90	65.87 ± 3.80	70.99 ± 4.53	13.45 ± 13.47	21.45 ± 14.38	50.74 ± 19.27
Reirradiation (3)	50.40 ± 0	39.64 ± 8.56	51.20 ± 2.56	56.09 ± 0.75	—	—	—

*Mean ± SD.

exposure portal films were obtained by dismounting the MIMiC device and double exposing the trip portal film with a 30 × 30 cm^2 open field at the same gantry angle (Fig 3b). A similar process was repeated at consecutive couch positions other than the origin to cover the entire target volume.

The detail of quality assurance process was described by Low et al. [10]. In brief, physicists performed and supervised quality assurance tests prior to each set of treatments. This included performing the following functions:

- Quality assurance procedures for installing the MIMiC prior to each fractionated treatment.
- MIMiC pattern test documenting that the pattern of the MIMiC was identical to the pattern intended for that gantry angle as displayed on printouts from the Peacock computer for a minimum of one gantry angle per arc (couch index).
- Dosimetry verification test using Peacock or Washington University anthropomorphic phantom in the same type of immobilization device as used in the patient. Films and/or thermoluminescent dosimeters (TLDs) and ionization chambers were placed in target and normal tissue phantom areas chosen from the treatment plan and specified the relationship to the surface reference point and/or the origin of the treatment plan. The measurements were reviewed by the treating physician before treatment proceeded.

Optimization of Treatment Plan

In traditional 3D CRT treatment planning, targets and organs at risk are contoured, and beam's-eye view displays are used to determine beam orientations. Appropriate beam weights are adjusted, and, if needed, beam modulators, such as wedges and compensating filters, are used. IMRT treatment planning also defines the target volume and organs at risk; however, instead of beams being designed the inverse planning dose constraints and previously described input parameters are specified. The selection of these parameters is not straightforward, and experience in their effect on the resulting dose distribution is essential. Because inverse planning allows the clinician the ability to designate desired doses to different targets and normal structures, selecting appropriate planning parameters as described above is critical to a best-achievable plan. Structure "weight" and "target priority" are highly individualized and may significantly affect the optimization of dose prescription. Our initial IMRT experience is described here.

RESULTS

Dose Delivered to the Targets

Table 3 shows the prescribed and delivered doses to the primary target and parotid gland. The mean of prescribed doses in patients with gross tumor, for postoperative treatment, and for reirradiation were 70.48, 64.18, and 50.40 Gy, respectively. Minimum doses to the targets ranged from 39.64–44.77 Gy. The mean volume of the targets receiving less than 95% prescription dose was 3% ± 1.4%. These dose points were generally located adjacent to critical structures, such as the spinal cord, brain stem, or parotid gland. The mean doses to the target satisfactorily met the prescription. In the meantime, the system has allowed the mean dose to the parotid gland to be around 20 Gy.

Treatment Tolerance and Acute Toxicity

In our experience, the noninvasive immobilization mask was well tolerated and yielded satisfactory reproducibility and accuracy [10,11]. All patients completed the prescribed treatment without unexpected treatment interruption. Acute confluent mucositis (Radiation Therapy Oncology Group Grade 3) was observed in 11 patients. Five patients lost more than 10% of body weight; however, none of them required hospitalization. Acute side effects were comparable to those in patients treated with conventional beam arrangements during the same period. At the 3-month follow-up visit, patients treated with irradiation only had recovered from radiation-related skin or mucosa side effects. Subjective assessment of xerostomia during radiation treatment and at 6 months after the completion of IMRT was performed in 14 patients who had not received radiation before. During radiation therapy,

Table 4. Tumor Control

Target characteristics	Local recurrence	Distant metastases	Disease-free
Gross tumor (8 patients)	0	0	8
Reirradiation (3 patients)	2	0	1
Postoperative (6 patients)	0	1	5

RTOG Grade 3 xerostomia was found in one patient with nasopharyngeal cancer. Eight patients experienced Grade 2 xerostomia, and four patients had Grade 1 symptoms. At 6 months after radiation, no patient showed RTOG Grade 3 xerostomia. Six patients still had Grade 2 xerostomia, and the six patients had only Grade 1 symptoms. The remaining two patients have no complaint of dry mouth.

Tumor Response

In 11 patients with gross tumor or reirradiation, complete response was achieved in nine (Table 4). One patient with a tonsillar primary tumor who presented with a cervical lymph node greater than 10 cm showed residual induration in the tumor bed, and a follow-up MRI scan revealed minimal enhancement consistent with postirradiation fibrosis. Two patients presented with T4 nasopharyngeal carcinoma extending into the cavernous sinus causing cranial nerve deficit; they have shown drastic improvement of their neurological symptoms. A follow-up MRI indicated greater than 80% reduction of tumor on a 4-month follow-up scan. There was no evidence of tumor recurrence at 12-month follow-up in the six patients treated in the adjuvant setting. One patient with a history of coronary artery disease died of a heart attack 2 months after the completion of irradiation. Among three patients who received IMRT for recurrent disease within previous high-dose irradiation regions, significant symptomatic relief has been achieved. Although two patients still had radiological evidence of disease, they remained alive 12 months after treatment. No recurrence was noted in the region receiving a daily fraction size of less than 1.9 Gy.

Optimization Results

Because target coverage and parotid sparing are two of the major concerns in conformal planning of head and neck cancer treatment, we studied the influence of optimization parameters (the structure weight and target priority) on dose distributions in the region between the parotid gland and targets. Six plans were generated, as shown in Figure 4, each with a common target weight of 1.0, but with variations in the parotid gland weight (0.5, 1, 2) and target priority (Yes or No). The target growth was

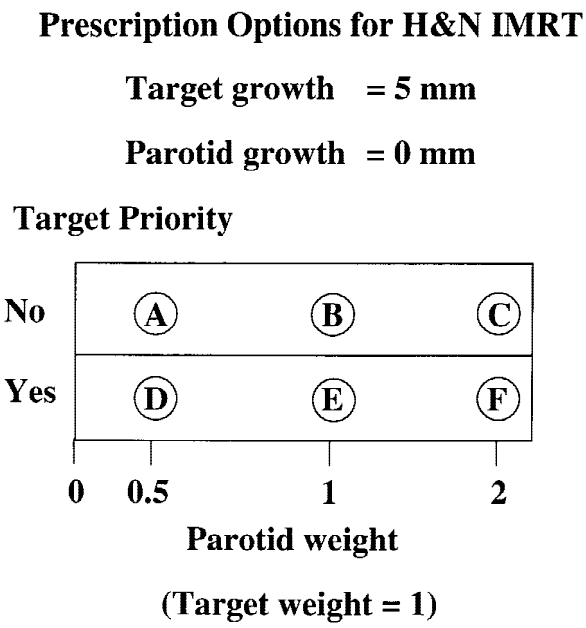

Fig. 4. Parameters in the inverse planning of intensity-modulated radiation therapy were studied to optimize the plan for parotid sparing.

5 mm, and no growth was placed on the parotid gland. Prescription was set to deliver 70 Gy to the target and 30 Gy to parotid gland. The target coverage and parotid gland dose were studied. As shown in Figure 5a,b, two quantities were evaluated: the fraction of the target volume receiving less than 95% of the prescription dose and the fraction of the parotid volume receiving more than 30 Gy.

Target priority had the most significant impact on target coverage. We found that Plans A–C (target did not have priority with increasing order of parotid weight) had significantly poorer coverage of the target volume than Plans D–F (target had priority with increasing order of parotid weight). However, the trade-off for better target coverage was a bigger volume of the parotid gland receiving a higher dose. For example, Plan D provided the best target coverage (<2% of target receiving <95% of prescription dose); however, nearly 50% of parotid glands received more than 30 Gy. In contrast, Plan C spared the parotid gland most effectively (only 14% of parotid glands received more than 30 Gy), but 7% of the target volume received less than 95% of the prescribed dose. The area of undercoverage was usually located in the junction of the target and parotid volume where the dose transition took place. This dose gradient at the edge of the target volume and the adjacent critical normal tissue is a common feature of IMRT dosimetry.

We also found that increasing parotid weight

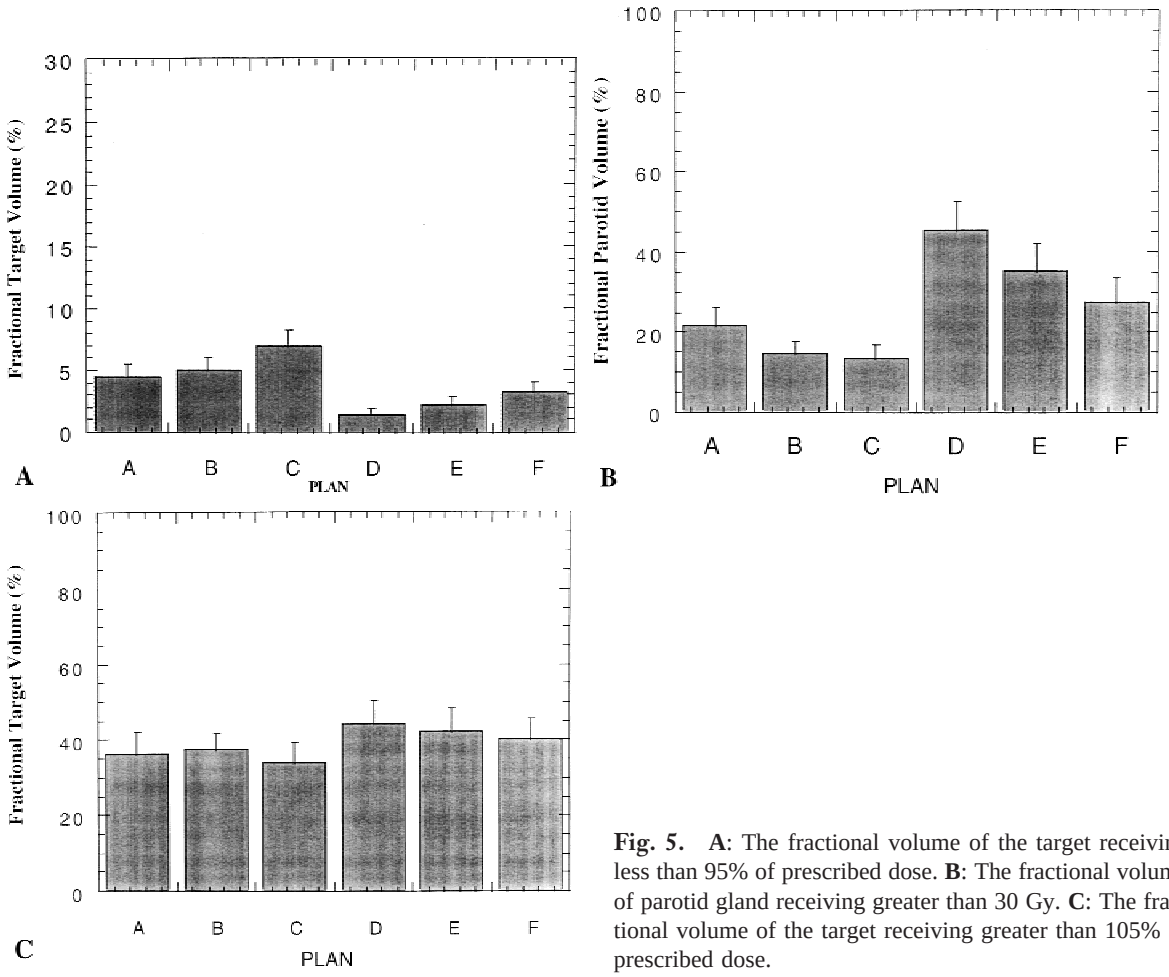

Fig. 5. **A**: The fractional volume of the target receiving less than 95% of prescribed dose. **B**: The fractional volume of parotid gland receiving greater than 30 Gy. **C**: The fractional volume of the target receiving greater than 105% of prescribed dose.

during inverse planning could improve parotid sparing without significantly compromising target coverage. As shown in Figure 5a,b, plans with higher parotid weight (Plans C and F) consistently yielded a smaller overdosed parotid gland volume than those with lower parotid weight (Plans A and D).

We further investigated dose inhomogeneity within the target volume to see whether increased conformality to the parotid gland would lead to a worse dose inhomogeneity within the target volume. The fraction of target volumes receiving this minimum dose was small and often occurred in the area adjacent to the parotid gland or other critical structures. In line with this finding, we also noted similar fractional target volumes receiving more than 105% dose in all six plans (Fig. 5c). These results suggested that the conformity for parotid sparing did not increase the fraction of target volume being treated to a higher dose.

Figure 6 shows the representative axial, coronal, and sagittal dose displays of a patient with nasopharyngeal carcinoma treated with this tomotherapy-based IMRT. Figure 7 illustrates the magnified view of the resulting isodose curves in the parotid region. The best plan with respect to parotid sparing was Plan C, in which the target did not have priority over the parotid gland and therefore yielded the worst target coverage, with 7% ± 1.3% of the target volume receiving less than 95% of the prescription dose. In contrast, when the target was prioritized the minimum doses to the target volume in Plans D–F were not different (ranging from 30.6–35.2 Gy), and the fractional volume of the target receiving less than 95% of prescription dose was significantly less than in Plans A–C. The best compromise seemed to be achieved by Plan F, which yielded one of the lowest target underdose volumes (3.3% ± 0.6%), with a relatively low fractional volume of parotid gland being overdosed (27% ± 8%).

DISCUSSION

A 3D CRT technique that can deliver the intended radiation dose to the target while sparing surrounding normal tissue for head and neck cancers is un-

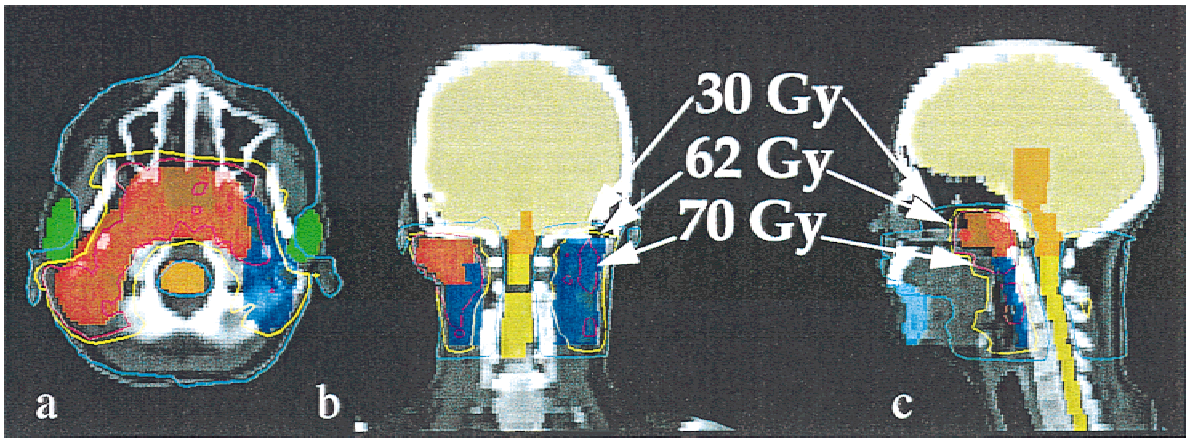

Fig. 6. The representative axial (**A**), coronal (**B**), and sagittal (**C**) dose displays in a patient with nasopharyngeal carcinoma treated with tomotherapy-based intensity-modulated radiation therapy.

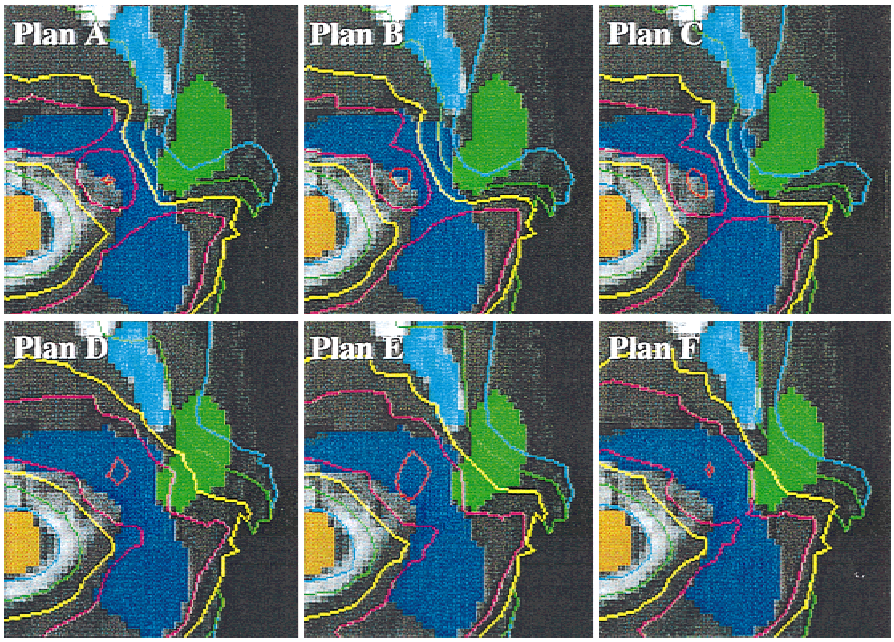

Fig. 7. A composite magnified view of the resulting isodose curves in the junctional region indicates the best plan (Plan C) with respect to parotid sparing yields the worst target coverage. Plan F seems to be the best compromise.

der relentless pursuit. The concept was sparked by a pilot investigation of Leibel et al. [12], who documented improvement in target coverage and normal tissue sparing when nasopharyngeal tumors were boosted using 3D planning compared with standard planning. Currently, several 3D CRT techniques are available, including the use of multiple coplanar or noncoplanar beam arrangements and intensity modulation with compensators. Eisbruch et al. [13] reported their initial experience in 15 head and neck cancer patients treated with a multiple-beam conformal plan to spare one side of the parotid gland. The technique was performed by using beam's-eye view displays and generating isodoses following each step. This forward-planning system was the first attempt to spare salivary function using 3D CRT. However, the planning process required the generation of multiple plans to select the best available and could be tedious and time-consuming. In addition, the resulting isodose plans had relatively large dose inhomogeneities despite manual optimization efforts.

To improve the dose distribution while reducing efforts in treatment design, we are implementing a user-friendly computer-aided IMRT optimization that determines the number and characteristics of the beams. With IMRT, as the beam is oriented around the patient the beam intensity (flu-

ence) is optimized using computer algorithms that consider the target and normal tissue dimensions and user-defined constraints such as dose limits. This process is referred to as the "inverse problem solution" or "inverse method" of treatment planning, which allows the radiation oncologist to 1) plan and evaluate sophisticated conformal plans, 2) improve geometric precision in patient treatment, 3) determine the clinical dose–volume constraints of normal tissue tolerance, and 4) investigate tumor response at various dose levels and fraction sizes [3,4,14–16].

IMRT can be delivered with a dynamic multileaf collimator or rotating contiguous arc beams. We implemented the latter technique in the Head and Neck IMRT Program at Washington University. We currently reserve this tomotherapy-based IMRT for tumors with a concave shape and those in close proximity to sensitive structures when high-dose irradiation is to be administered. Head and neck cancer is an ideal disease site for the application of this promising technology [16–18]. This technique is more complex and staff time and effort is greater than with conventional techniques. A recent study at our institution showed that treatment planning time including 3D simulation is about 4 hr and daily treatment sessions are 35 min (in contrast to 2 hr planning and 15 min daily treatment time with conventional irradiation) [19]. The IMRT delivery and planning system will continue to evolve and efficiency will be improved. However, regardless of which planning system is used the objectives of optimization must be specified and must be clinically relevant. In this study, the salivary gland was selected as the model critical normal tissue to demonstrate the merit of each prescription plan. Radiation causes changes to the salivary glands, especially to the serous cells, resulting in a reduction in salivary output and a change in the viscosity of saliva. The degree of permanent dry month (xerostomia) depends on the volume of the salivary gland included in the irradiation field and the dose delivered to that volume. Even low doses of radiation cause changes in the quantity and quality of salivary flow [20–22]. This is particularly true for the parotid gland, since it is the largest of the major salivary glands, is the main source of alkaline and serous secretions, and is very sensitive to radiation injury [22–26]. Most of the prior investigations of salivary gland tolerance in humans were performed before the introduction of 3D CRT techniques. Because of the lack of dose–volume information, the main focus was on whole-organ damage after a high dose (40–60 Gy) of irradiation. This information is valuable but may not be applicable in the current era of 3D CRT, with which sparing of a substantial volume of the salivary gland to a much lower dose is possible. Because the degree of xerostomia depends on both the radiosensitivity of salivary gland tissue and the fraction of functional salivary subunits irradiated, parotid gland dose-volume information was used to address the merit of each individual plan [27]. The selection of these optimization parameters may not be straightforward and varies in different planning systems; gaining experience in their influence on the resulting dose distribution is a critical step before any clinical application. Furthermore, we are aware that a small fraction of the target volume in the junctional region was underdosed as one of the consequences of parotid sparing. Its clinical significance is under close scrutiny.

Patient motion between sequential arc deliveries in tomotherapy-based IMRT could yield dose heterogeneity at the gradient of 10%/mm [28]. Patient immobilization is therefore extremely important. We are using a noninvasive immobilization system as shown in Figure 1. This system has been accepted well by our patients and treating technologists. To verify the reproducibility of daily setup of patients, we invented a double-exposure portal film technique that allows a representative arc-strip to be shown with the anatomy of the head and neck. This double-exposure portal film was used to compare against the corresponding DRRs, as shown in Figure 3. The accuracy of patient positioning was determined by manually marking bony landmarks and overlaying the portal films and DRRs. If necessary, adjustments were made before the initiation of treatment. In our preliminary experience, this noninvasive immobilization system yielded high reproducibility [11]. This is in concordance with Verellen et al. [16,18], who reported their initial satisfactory experience in patients with head and neck tumors using a noninvasive mask for IMRT treatment. It is also compatible with the results of invasive immobilization head screws [15]. Although in our initial experience we have not encountered patients with significant weight loss during treatment that leads to significant immobilization variation, it is advisable that the mask be remade and plans be rerun for patients with drastic changes in weight and tumor size to ensure adequate immobilization.

In conventional planning for head and neck cancers, patients are often treated with a cone-down boost technique to deliver different dose levels to various targets. The initial and boost portals are delivered sequentially, often with the same daily fraction dose. To mimic the conventional fraction dose scheme, at least two IMRT plans (one for

initial large field and another for the boost) must be generated per patient during a course of treatment. This will require an integration of dose-volume information from at least two IMRT plans to yield the composite DVH of each individual target and critical structure in the inverse planning system. The currently available planning system does not possess such a feature. Therefore, we took the alternative approach to deliver different doses to selected segments of the tumor target volume (i.e., gross tumor vs. microscopic neck nodes) by adjusting the daily fraction dose using the linear-quadratic model. For each target, a BED was computed to adjust for the areas receiving a daily fraction dose of less than 1.9 Gy. We elected to limit the reference fraction size to 1.9 Gy because concurrent chemotherapy is increasingly used in the management of head and neck cancers. Escalating the daily fraction dose to the gross tumor while maintaining 1.9 Gy to the target containing microscopic disease is an attractive alternative because overall treatment time will be shortened. However, late side effects may increase, especially when concurrent chemotherapy is given.

CONCLUSIONS

The driving force that inspired pursuit of CRT for head and neck cancer is based on the concept that therapeutic gain can be optimized if one can deliver the prescribed dose to the target tumor volume while minimizing radiation damage to the neighboring normal tissues. A system for patient immobilization, setup verification, and dose optimization of parotid sparing without significantly compromising target coverage is being implemented for tomotherapy-based IMRT at the Mallinckrodt Institute of Radiology. Initial clinical experience is promising, and no severe adverse acute side effects have been observed. Although the planning and delivery of IMRT are more complex than those of traditional beam arrangements, IMRT can achieve a higher degree of target conformity, especially for target volumes with complex (concave) geometry, which is a common feature of head and neck cancers. Further refinement of delivery technology and the inverse planning system, gaining clinical experience to address target definition and dose inhomogeneity within the targets, and understanding the partial volume effect on normal tissue tolerance will help to promote the prevalence of IMRT [29,30].

ACKNOWLEDGMENT

This work was supported in part by a corporate grant from the Nomos Corporation.

REFERENCES

1. Parker S, Tong T, Bolden S, Wingo P. Cancer statistics, 1997. CA Cancer J Clin 1997;47:5–27.
2. Emami B, Lyman J, Brown A. Tolerance of normal tissue to therapeutic irradiation. Int J Radiat Oncol Biol Phys 1991;21:109–122.
3. Purdy JA. Advances in three-dimensional treatment planning and conformal dose delivery. Semin Oncol 1997;24:655–671.
4. Carol MP. Integrated 3D conformal planning/multivane intensity modulating delivery system for radiotherapy. In: Purdy JA, Emami B, editors. 3D radiation treatment planning and conformal therapy. Madison, WI: Medical Physics Publishing; 1995. p 435–445.
5. ICRU #50. Prescribing, recording, and reporting photon beam therapy. International Commission on Radiation Units and Measurements, Washington, DC: ICRU, 1993.
6. Hayman LA, Taber KH, Diaz-Marchan PJ, Stewart MG, Malcolm ML, Laine FJ. Spatial compartments of the neck. III. Axial sections. Int J Neuroradiol 1998;4: 393–402.
7. Dale GRG. The application of the linear-quadratic dose-effect equation for fractionated and protracted radiotherapy. Cancer 1985;75:2351–2355.
8. Al-Sarraf M, LeBlanc M, Giri PGS. Chemoradiotherapy versus radiotherapy in patients with advanced nasopharyngeal cancer: Phase III randomized intergroup study 0099. J Clin Oncol 1998;16:1310–1317.
9. Brizil DM. Radiotherapy and concurrent chemotherapy for the treatment of locally advanced head and neck squamous cell carcinoma. Semin Radiat Oncol 1998;8: 237–246.
10. Low DA, Mutic S, Dempsey JF, Markman J, Goddu SM, Purdy JA. Abutment region dosimetry for serial tomotherapy. Int J Radiat Oncol Biol Phys (in press).
11. Chao KSC, Low DA, Gerber RL, Perez CA, Purdy JA. Clinical and technical considerations for head and neck cancers treated by IMRT (Abst.). Int J Radiat Oncol Biol Phys 1997;39(Suppl):238.
12. Leibel SA, Kutcher GJ, Harrison LB. Improved dose distributions for 3D conformal boost treatments in carcinoma of the nasopharynx. Int J Radiat Oncol Biol Phys 1991;20:823–833.
13. Eisbruch A, Ship JA, Martel MK. Parotid gland sparing in patients undergoing bilateral head and neck irradiation: techniques and early results. Int J Radiat Oncol Biol Phys 1996;36:469–480.
14. Meeks SL, Buatti JM, Bova FJ, Friedman WA, Mendenhall WM, Zlotecki RA. Potential clinical efficacy of intensity-modulated conformal therapy. Int J Radiat Oncol Biol Phys 1998;40:483–495.
15. Tsai JS, Wazer DE, Ling MN. Dosimetric verification of the dynamic intensity-modulated radiation therapy of 92 patients. Int J Radiat Oncol Biol Phys 1998;40: 1213–1230.
16. Verellen D, Linthout N, Storme G. Target localization and treatment verification for intensity modulated conformal radiation therapy of the head and neck region: the AZ-VUB experience. Akademisch Ziekenhuis-

Vrije Universiteit Brussel. Strahlenther Onkol 1998; 174(Suppl 2):19–27.
17. Boyer AL, Geis P, Grant W, Carol M. Modulated beam conformal therapy for head and neck tumors. Int J Radiat Oncol Biol Phys 1997;39:227–236.
18. Verellen D, Linthout N, van den Berg D, Bel A, Storme G. Initial experience with intensity-modulated conformal radiation therapy for treatment of the head and neck region. Int J Radiat Oncol Biol Phys 1997;39:99–114.
19. Perez CA, Kobeissi BJ, Chao C. Cost benefit of three-dimensional conformal or intensity modulated irradiation. 3-D conformal radiation therapy and intensity modulated radiation therapy in the new millennium. Houston, TX; Baylor College of Medicine, Office of Continuing Medical Education; 1999, Section 10.
20. Kashima HK, Kirkham WB, Andrews JR. Postirradiation sialadenitis: a study of the clinical features, histopathlogic changes and serum enzyme variations following irradiation of human salivary glands. Am J Roentgenol Rad Ther Nucl Med 1965;94:271–291.
21. Parsons JT. The effect of radiation on normal tissues of the head and neck. In: Million RR, Cassisi NJ, editors. Management of head and neck cancer. Philadelphia: JB Lippincott, 1984. p 173–207.
22. Shannon IL. Management of head and neck irradiated patients. In: Zelles T, editor. Advances in physiological science, saliva and salivation. New York: Pergamon; 1978. p 313–322.
23. Cheng VST, Downs J, Herbert D, Aramany M. The function of the parotid gland following radiation therapy for head and neck cancer. Int J Radiat Oncol Biol Phys 1981;7:253–258.
24. Stephens LC, Ang KK, Schultheiss TE, King GK, Brock WA, Peters LJ. Target cell and mode of radiation injury in rhesus salivary glands. Radiother Oncol 1986; 7:165–174.
25. Stephens LC, King GK, Peters LJ, Ang KK, Schultheiss TE, Jardine JH. Acute and late radiation injury in rhesus monkey parotid glands: evidence of interphase cell death. Am J Pathol 1986;124:469–478.
26. Tsujii H. Quantitative dose-response analysis of salivary function following radiotherapy using sequential Ri-sialography. Int J Radiat Oncol Biol Phys 1985;11: 1603–1612.
27. Wang XH, Mohan R, Jackson A, Leibel S, Fuks Z, Ling CC. Optimization of intensity-modulated 3D conformal treatment plans based on biological indices. Radiother Oncol 1995;37:140–152.
28. Carol M, H. GW, Blier AR. The field-matching problem as it applies to the Peacock three dimensional conformal system for intensity modulation. Int J Radiat Oncol Biol Phys 1996;34:183–187.
29. Burman C, Chui CS, Kutcher G. Planning, delivery, and quality assurance of intensity-modulated radiotherapy using dynamic multileaf collimator: a strategy for large-scale implementation for the treatment of carcinoma of the prostate. Int J Radiat Oncol Biol Phys 1997;39:863–873.
30. Woo SY, Grant WH, Bellezza D. A comparison of intensity modulated conformal therapy with a conventional external beam stereotactic radiosurgery system for the treatment of single and multiple intracranial lesions. Int J Radiat Oncol Biol Phys 1996;35:593–597.